



Density matrix numerical renormalization group for non-Abelian symmetries

A. I. Tóth,^{1,2} C. P. Moca,^{1,3} Ö. Legeza,^{1,4} and G. Zaránd¹

¹*Department of Theoretical Physics, Institute of Physics, Budapest University of Technology and Economics, H-1521 Budapest, Hungary*

²*Institute for Theoretische Festkörper Physik, Universität Karlsruhe, D-76128 Karlsruhe, Germany*

³*Department of Physics, University of Oradea, 410087 Oradea, Romania*

⁴*Research Institute for Solid State Physics and Optics, P.O. Box 49, H-1525 Budapest, Hungary*

(Received 22 May 2008; published 8 December 2008)

We generalize the spectral sum rule preserving density matrix numerical renormalization group (DM-NRG) method in such a way that it can make use of an arbitrary number of not necessarily Abelian local symmetries present in the quantum impurity system. We illustrate the benefits of using non-Abelian symmetries by the example of calculations for the T matrix of the two-channel Kondo model in the presence of magnetic field, for which conventional NRG methods produce large errors and/or take a long run-time.

DOI: [10.1103/PhysRevB.78.245109](https://doi.org/10.1103/PhysRevB.78.245109)

PACS number(s): 71.10.Pm, 71.27.+a, 72.15.Qm, 73.21.La

I. INTRODUCTION

Quantum impurity models play a crucial role in our understanding of strongly correlated systems: they appear in the description of correlated mesoscopic structures,¹ they show up in molecular electronics, and many of the properties of correlated bulk systems can also be accounted for using self-consistent quantum impurity models within the dynamical mean-field approach.² Despite a lot of interest and the large amount of effort invested in understanding these models, we have, unfortunately, very limited tools to describe quantitatively the general properties of a generic quantum impurity model. For some of the quantum impurity models Bethe ansatz,^{3,4} conformal field theory,⁵ bosonization,⁶ perturbative calculations,^{7,8} or a Fermi-liquid theory⁹ can provide a satisfactory explanation. However, these results are usually restricted to some regions in the parameter space. Therefore, even today, the most reliable method to obtain accurate information on a generic quantum impurity model over the whole parameter space and for any frequency is Wilson's numerical renormalization group (NRG) (Ref. 10) method originally developed for the one-channel Kondo model (1CKM).

Apart from being extended to compute dynamical properties,^{11–14} Wilson's method has been used in its original form for a long time, and it is only recently that this method has been further developed using some concepts similar to the ones in the density matrix renormalization group (DMRG) method.¹⁵ First, Hofstetter¹⁶ realized that a density matrix numerical renormalization group (DM-NRG) procedure needs to be introduced in certain cases to avoid spurious results. The method of Hofstetter, however, applied the original truncation scheme of Wilson, and therefore has not conserved spectral weights. A remarkable development of the NRG scheme has been the introduction of a complete basis set by Anders and Schiller,¹⁷ which was used to develop the time-dependent DM-NRG algorithm, and it also led to the development of spectral sum-conserving DM-NRG algorithms.^{18,19} In the work of Weichselbaum and von Delft,¹⁹ the spectral sum-conserving method has been formulated in the language of matrix product states.

Using symmetries is an important element of NRG. For the simplest models, it is usually sufficient to use Abelian

symmetries. However, for the more interesting two-channel and multichannel models it is crucial to exploit symmetries, since the computational effort needed increases rapidly with the number of electron channels, and it is very important to keep a sufficiently large number of levels in the DM-NRG procedure to achieve good accuracy. Despite the amazing development discussed in the previous paragraph, a general framework in which the advantages of non-Abelian symmetries are exploited in conjunction with DM-NRG was still missing, apart from the generalization of DM-NRG for the case of only one SU(2) symmetry.²⁰ Non-Abelian symmetries have been used extensively by the DMRG community.^{21,22} There, however, one always works with an incomplete set of states. The aim of the present paper is to develop a general scheme and to show how the spectral sum-conserving DM-NRG method can be used in combination with non-Abelian symmetries. Using such symmetries is very important for many quantum impurity models to speed up the numerical computation and to increase the size of the Hilbert space to achieve sufficient accuracy. For this purpose, we derive a very general recursion formula for the reduced density matrix. We shall show how this formula can be used to evaluate the spectral function of any retarded Green's function of the form

$$G_{A,B}^R(t) \equiv -i\langle [A(t), B(0)]_{\xi} \Theta(t) \rangle. \quad (1)$$

Here A and B are any kind of local fermionic or bosonic operators acting at the impurity site and $[A, B]_{\xi} = AB - \xi BA$ denotes the commutator ($\xi=1$) and the anticommutator ($\xi=-1$) for bosonic or fermionic operators, respectively. In Eq. (1), $\langle \dots \rangle$ denotes the average with the equilibrium density matrix, $\langle \dots \rangle = \text{Tr}\{\dots \rho\}$. Expressions for static quantities shall also be derived.

Due to the general recursion relation mentioned above, we are able to perform DM-NRG calculations independently of the number and type of discrete and compact Lie group symmetries considered and build a completely flexible DM-NRG code that handles symmetries dynamically and “blindly.”²³

To demonstrate the benefits of our procedure, we shall present numerical results for the two-channel Kondo (2CK)

model, which is the most basic non-Fermi-liquid quantum impurity model²⁴ and provides an excellent testing ground for multiple non-Abelian symmetries. Furthermore, its study is also motivated by its recent mesoscopic realization in double-dot systems by Potok *et al.*²⁵ As we shall see, conventional NRG techniques and DM-NRG with Abelian symmetries give rather poor results compared to a computation performed using the nontrivial symmetry structure of the model.

The paper is organized as follows. In Sec. II we present how one can exploit the internal symmetries of the quantum impurity system in the NRG process. In Sec. III the general procedure, which permits the use of an arbitrary number of local symmetries, is extended to the spectral sum rule preserving DM-NRG algorithm. In Sec. IV we provide the general formulas for computing Green's functions in the DM-NRG framework using symmetries. In Sec. V we present our numerical results for the local fermions' and local composite fermions' spectral functions and for the on-shell T matrix in the two-channel Kondo model which strongly support the use of DM-NRG (with the largest possible symmetry of the system) as opposed to the use of NRG. In Sec. VI we summarize our results. The formalism introduced in Sec. II is rather abstract. Therefore, to make it more accessible to the reader, in Appendix A we demonstrate how it operates through the example of the single-channel Kondo model. In Appendix B we give an alternative derivation of the result that the reduced density matrix retains its diagonal form in the course of the reduction for the special case when the symmetry contains only SU(2) groups from among non-Abelian ones.

II. ROLE OF SYMMETRIES IN THE NRG PROCEDURE

In this section we discuss how non-Abelian symmetries appear in the density matrix NRG calculations. In many cases, including these symmetries is essential for increasing the size of the truncated Hilbert space and thus obtaining results of high accuracy. We start with setting up a general formalism in which we then describe the diagonalization procedure and give the recursion relations needed for the diagonalization of the Wilson chain. To give a specific example, in Appendix A we present the analysis of the symmetries of the single-channel Kondo model within the general framework presented here in Sec. II.

A. Local symmetries on the Wilson chain

To set the notation, let us briefly present some symmetry considerations applied to Hamiltonians of the form

$$H = \mathcal{H}_0 + \sum_{n=0}^{\infty} (\tau_{n,n+1} + \mathcal{H}_{n+1}). \quad (2)$$

Here \mathcal{H}_0 contains the interaction between the impurity and the fermionic bath (the site of the impurity is labeled by 0), and nearest neighbors on the Wilson chain are coupled through the hopping terms $\tau_{n,n+1}$. The n th on-site term \mathcal{H}_{n+1} describes local correlations or interactions, and it can also account for the absence of the electron-hole symmetry.

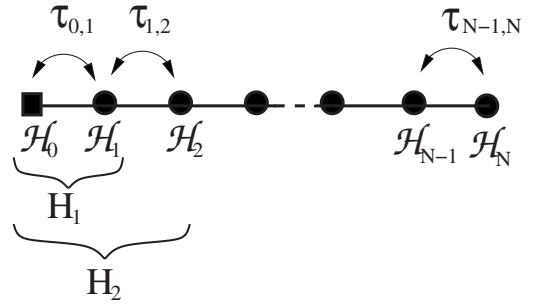


FIG. 1. Construction of the Hamiltonian on the Wilson chain of length N . The impurity sits at the square-shaped site labeled by 0; dots represent further sites. At the zeroth NRG iteration H_0 is identical with \mathcal{H}_0 . As the n th site is added to the chain, H_n is constructed recursively from the hopping term ($\tau_{n-1,n}$), from the on-site energy (\mathcal{H}_n), and from H_{n-1} .

NRG solves model (2) by an iterative diagonalization process.¹⁰ The iteration steps consist of diagonalizing the set of Hamiltonians introduced recursively by

$$H_0 = \mathcal{H}_0, \quad (3)$$

$$H_n = H_{n-1} + \tau_{n-1,n} + \mathcal{H}_n. \quad (4)$$

This recursion is depicted in Fig. 1.

Let us now assume that H , as well as every H_n , is invariant under the group G , i.e.,

$$\mathcal{U}(g)H_n\mathcal{U}^{-1}(g) = H_n, \quad n = 0, 1, 2, \dots \quad (5)$$

holds for every $g \in G$, with $\mathcal{U}(g)$ as the appropriate unitary operator. Furthermore, let us suppose that G and correspondingly \mathcal{U} can be decomposed into a direct product of Γ subgroups \mathcal{G}_γ ($\gamma = 1, \dots, \Gamma$), each acting independently on every lattice site,

$$G = \mathcal{G}_1 \times \mathcal{G}_2 \times \dots \times \mathcal{G}_\Gamma, \quad (6)$$

$$\mathcal{U}(g) = \prod_{\gamma=1}^{\Gamma} \mathcal{U}_\gamma(g_\gamma) = \prod_{\gamma=1}^{\Gamma} \prod_n \mathcal{U}_{\gamma,n}(g_\gamma). \quad (7)$$

This decomposition property is crucial for using symmetries in the NRG calculations.

Note that in the considerations above the subgroups can be also finite, and \mathcal{G}_γ can represent a crystal field symmetry as well as, e.g., the SU(3) group. However, some of the considerations presented in this paper may not apply to non-compact groups.

The above decomposition is not necessarily unique. Nevertheless, having obtained a specific decomposition, the irreducible subspaces (multiplets) of the Hamiltonians H_n can be classified by a total of Γ quantum numbers,

$$\underline{Q} = \{Q^1, Q^2, \dots, Q^\Gamma\}, \quad (8)$$

and, by analogy to SU(2), states within the multiplets are labeled by the internal quantum numbers,²⁶

$$Q^z = \{Q^{1,z}, Q^{2,z}, \dots, Q^{\Gamma,z}\}. \quad (9)$$

We use the convention that every multiplet in the spectrum is labeled by a separate label, i , and that the quantum numbers of the multiplet are viewed as a function of i , \underline{Q}_i .²⁷ Therefore the quantum numbers \underline{Q}_i could, in principle, be removed from the labels of a state, i.e., $|i, \underline{Q}_i \underline{Q}_i^z\rangle \rightarrow |i, \underline{Q}_i^z\rangle$, since \underline{Q}_i is determined uniquely by the multiplet label i itself. However, to be more explicit, we keep this somewhat redundant label in what follows.

We shall refer to the quantum numbers \underline{Q}_i as *representation indices*, while \underline{Q}_i^z are referred to as *labels* of the internal basis states of a given multiplet. Note that the dimension of the i th subspace depends uniquely on its quantum numbers \underline{Q}_i , i.e.,

$$\dim(i) \equiv \dim(\underline{Q}_i) = \prod_{\gamma=1}^{\Gamma} \dim(Q_i^\gamma), \quad (10)$$

where $\dim(Q_i^\gamma)$ is the dimension of an irreducible representation characterized by the representation index Q_i^γ (cf. Appendix A).

Operators can be arranged into irreducible tensor operators, and an irreducible tensor operator multiplet A is correspondingly described by quantum numbers \underline{a} , while members of the multiplet are labeled by \underline{a}^z with \underline{a} and \underline{a}^z being Γ -component vectors.²⁸ The Wigner-Eckart theorem^{28,29} tells us that—apart from trivial group theoretical factors (Clebsch-Gordan coefficients)—the matrix elements of the members of a given operator multiplet and states within two multiplets i and j are related by

$$\langle i, \underline{Q}_i \underline{Q}_i^z | A_{\underline{a}, \underline{a}^z} | j, \underline{Q}_j \underline{Q}_j^z \rangle = \langle i | | A | | j \rangle \langle \underline{Q}_i \underline{Q}_i^z | \underline{a} \underline{a}^z; \underline{Q}_j \underline{Q}_j^z \rangle, \quad (11)$$

where $\langle i | | A | | j \rangle$ denotes the reduced (invariant) matrix element of A , and the generalized Clebsch-Gordan coefficients are simply defined as

$$\langle \underline{Q}_i \underline{Q}_i^z | \underline{a}^z \underline{a}^z; \underline{Q}_j \underline{Q}_j^z \rangle \equiv \prod_{\gamma=1}^{\Gamma} \langle Q_i^\gamma \underline{Q}_i^{\gamma,z} | \underline{a}^\gamma \underline{a}^{\gamma,z}; Q_j^\gamma \underline{Q}_j^{\gamma,z} \rangle$$

with the usual Clebsch-Gordan coefficients²⁸ on the right-hand side. This relation is used extensively in the NRG calculations.

B. Role of symmetries in the diagonalization procedure

Before discussing NRG with a complete basis set,¹⁷ let us shortly look into how symmetries are used in Wilson's NRG. In his original work, Wilson constructed iteratively approximate eigenstates of H_n for a chain of length n . However, in each iteration the dimension of the Hilbert space increases by a factor d , with d as the dimension of the local Hilbert space at a single site of the chain with site label $n > 0$. Therefore the size of the Hilbert space increases exponentially with n , and after a few iterations one must truncate it: some of the states i are therefore discarded ($i \in D$), while other states are kept ($i \in K$) and are used to construct approximate eigenstates for H_{n+1} . Symmetries are of great value in this diagonalization procedure: in their presence the H_n 's are block diagonal in the representation indices, and the eigenvalue problem can be solved much more efficiently. On the other

hand, using non-Abelian symmetries implies a larger number of effective kept states through the internal degeneracies of multiplets. For some of the physical quantities and impurity models, it is crucial to increase the number of kept states as much as possible to achieve good numerical accuracy. Therefore, for many applications it may be essential to use non-Abelian symmetries extensively.

In Wilson's original formulation of NRG, symmetries are used in the following way: as discussed above, in the n th iteration the eigenstates (multiplets) of H_n are constructed from the kept multiplets labeled by u with $u \in K$ of the $(n-1)$ th iteration, which are approximate low-energy eigenstates of H_{n-1} , and from a complete set of *local states* (multiplets) labeled by μ that live at the n th site. In the following, we refer to these new approximate eigenstates \tilde{i} as *new states*, while by analogy with DMRG, we shall call the kept states *block states* or *old states*.

In the presence of symmetries, each new multiplet carries representation indices $\underline{Q}_i = \{Q_i^\gamma\}$, and states within this multiplet are labeled by the internal quantum numbers $\underline{Q}_i^z = \{Q_i^{\gamma,z}\}$. Similarly, local states have quantum numbers $\underline{q}_\mu = \{q_\mu^\gamma\}$ and are further labeled by $\underline{q}_\mu^z = \{q_\mu^{\gamma,z}\}$. To construct the approximate eigenstates of H_n , we first construct new states from $|u, \underline{Q}_u \underline{Q}_u^z\rangle_{n-1}$ by adding electrons at site n ,

$$|u, \underline{Q}_u \underline{Q}_u^z\rangle_{n-1} \rightarrow |\mu, \underline{q}_\mu \underline{q}_\mu^z\rangle_{\text{loc}} \otimes |u, \underline{Q}_u \underline{Q}_u^z\rangle_n. \quad (12)$$

We then use the Clebsch-Gordan coefficients to build from the block (old) and local states (new) states that transform as irreducible multiplets under the symmetry transformations, $\mathcal{U}(g)$. From a given block state u and a local state μ we can form several new multiplets labeled by \tilde{i} by the following construction:

$$\begin{aligned} |\tilde{i}, \underline{Q}_i \underline{Q}_i^z\rangle_n &\equiv \sum_{\underline{Q}_u \underline{Q}_u^z} \langle \underline{Q}_i \underline{Q}_i^z | \underline{q}_\mu \underline{q}_\mu^z; \underline{Q}_u \underline{Q}_u^z \rangle^* |\mu, \underline{q}_\mu \underline{q}_\mu^z\rangle_{\text{loc}} \\ &\otimes |u, \underline{Q}_u \underline{Q}_u^z\rangle_{n-1}, \quad (\tilde{i} \leftarrow u, \mu \text{ with } u \in K). \end{aligned} \quad (13)$$

In this way, every new state \tilde{i} “remembers” its parent states. The multiplets of Eq. (13) shall be referred to as the *canonical basis* from now on. Since H_n is scalar under the group G , it has a block-diagonal structure, and the multiplets in Eq. (13) are irreducible by construction,

$${}_n \langle \tilde{i}, \underline{Q}_i \underline{Q}_i^z | H_n | \tilde{j}, \underline{Q}_j \underline{Q}_j^z \rangle = {}_n \langle \tilde{i} | | H_n | | \tilde{j} \rangle \delta_{\underline{Q}_i \underline{Q}_i^z, \underline{Q}_j \underline{Q}_j^z}. \quad (14)$$

Thus H_N is diagonalized by a block-diagonal unitary transformation, $\mathcal{O}_{i,i}^{[n]}$,

$$H_n |i, \underline{Q}_i \underline{Q}_i^z\rangle_n = E_i^n |i, \underline{Q}_i \underline{Q}_i^z\rangle_n, \quad (15)$$

$$|i, \underline{Q}_i \underline{Q}_i^z\rangle_n = \sum_{\tilde{i}} \mathcal{O}_{i,\tilde{i}}^{[n]} |\tilde{i}, \underline{Q}_i \underline{Q}_i^z\rangle_n \delta_{\underline{Q}_i \underline{Q}_i^z, \underline{Q}_{\tilde{i}} \underline{Q}_{\tilde{i}}^z}, \quad (16)$$

with E_i^n as the eigenenergies of H_n . Here \mathcal{O} is a block-diagonal matrix, and its columns in a given symmetry sector

are just the eigenvectors of the corresponding submatrix of ${}_n\langle\tilde{i}|H_n|\tilde{j}\rangle_n$ in the canonical basis. In the upcoming iteration, some of these multiplets shall be kept, typically those of lowest energy, and form the block states of the $(n+1)$ th iteration, while others are again discarded.

In the iteration step outlined above the matrix elements ${}_n\langle\tilde{i}|H_n|\tilde{j}\rangle_n$ are needed, with $H_n=H_{n-1}+\tau_{n-1,n}+\mathcal{H}_n$. The matrix elements of H_{n-1} follow simply from Eq. (13) and from the fact that the block states are the eigenstates of H_{n-1} . They are simply given by

$${}_n\langle\tilde{i}|H_{n-1}|\tilde{j}\rangle_n = E_u^{n-1} \delta_{\tilde{i},\tilde{j}}, \quad (17)$$

where u is the state from which state \tilde{i} has been constructed. Similarly, the matrix elements of \mathcal{H}_n are given by

$${}_n\langle\tilde{i}|\mathcal{H}_n|\tilde{j}\rangle_n = \varepsilon_\mu^n \delta_{\tilde{i},\tilde{j}}, \quad (18)$$

where ε_μ^n is just the expectation value of \mathcal{H}_n with local states within the multiplet μ . Finally, to compute the matrix elements of the hopping $\tau_{n-1,n}$, we use the fact that $\tau_{n-1,n}$ can always be decomposed as

$$\tau_{n-1,n} = \sum_\alpha h_\alpha^{[n-1]} \sum_{\underline{c}^z} [C_{\alpha;\underline{c},\underline{c}^z}^{[n-1]} (C_{\alpha;\underline{c},\underline{c}^z}^{[n]})^\dagger + \text{H.c.}]. \quad (19)$$

Here $C_{\alpha;\underline{c},\underline{c}^z}^{[n-1]}$ denotes some *creation operator multiplet* at site $n-1$ that has quantum numbers \underline{c} , and $h_\alpha^{[n-1]}$ are the hopping amplitudes between sites $n-1$ and n . The index α in the equation above labels various ‘‘hopping operators.’’ To give a simple example, if we treat the 1CKM using only U(1) symmetries we have two hopping operators, $\alpha \in \{1, 2\}$, corresponding to $C_1^{[n]} = f_{n,\uparrow}^\dagger$ and $C_2^{[n]} = f_{n,\downarrow}^\dagger$. However, if we use the spin SU(2) symmetry, then $\alpha=1$ and $C_1^{[n]} = \{f_{n,\uparrow}^\dagger, f_{n,\downarrow}^\dagger\}$.

For the reduced matrix elements of $\tau_{n-1,n}$, one obtains using Eq. (13) and the decomposition (19) the following formula:

$$\begin{aligned} {}_n\langle\tilde{i}|\tau_{n-1,n}|\tilde{j}\rangle_n &= \sum_\alpha h_\alpha^{[n-1]} {}_{n-1}\langle u|C_\alpha^{[n-1]}|v\rangle_{n-1\text{loc}} \langle v|C_\alpha^{[n]}|\mu\rangle_{\text{loc}}^* \\ &\times D(\alpha, \underline{c}, \underline{Q}_{\tilde{i}}, \underline{Q}_{\tilde{j}}, \underline{Q}_u, \underline{Q}_v, \underline{q}_\mu, \underline{q}_v) \delta_{\underline{Q}_{\tilde{i}}, \underline{Q}_{\tilde{j}}} \delta_{\underline{Q}_{\tilde{i}}, \underline{Q}_{\tilde{j}}}^z \\ &+ \text{H.c.}, \quad (\tilde{i} \leftarrow \mu, u; \tilde{j} \leftarrow v, v). \end{aligned} \quad (20)$$

Here the state \tilde{i} has been constructed from the kept state u of the previous iteration and from the local state μ , while \tilde{j} has been constructed from v and ν . The functions $D(\alpha, \underline{c}, \underline{Q}_{\tilde{i}}, \underline{Q}_{\tilde{j}}, \underline{Q}_u, \underline{Q}_v, \underline{q}_\mu, \underline{q}_v)$ denote group theoretical factors,

$$D(\alpha, \underline{c}, \underline{Q}_{\tilde{i}}, \underline{Q}_{\tilde{j}}, \underline{Q}_u, \underline{Q}_v, \underline{q}_\mu, \underline{q}_v) = \text{sgn}(C, \mu) \sum_{\underline{c}^z} \sum_{\underline{Q}_{\tilde{i}}, \underline{Q}_{\tilde{j}}, \underline{Q}_u, \underline{Q}_v} \langle \underline{Q}_{\tilde{i}} \underline{Q}_{\tilde{j}} | \underline{q}_\mu \underline{q}_\nu^z; \underline{Q}_u \underline{Q}_v \rangle \langle \underline{Q}_{\tilde{i}} \underline{Q}_{\tilde{j}} | \underline{q}_\nu \underline{q}_\nu^z; \underline{Q}_v \underline{Q}_v \rangle^* \langle \underline{Q}_u \underline{Q}_u | \underline{c} \underline{c}^z; \underline{Q}_v \underline{Q}_v \rangle \langle \underline{q}_\nu \underline{q}_\nu^z | \underline{c} \underline{c}^z; \underline{q}_\mu \underline{q}_\mu^z \rangle^* \quad (21)$$

with $\underline{Q}_{\tilde{i}}^z$ chosen arbitrarily. The sign function $\text{sgn}(C, \mu) = \pm 1$ arises as one commutes the creation operators implicitly present in the local state μ over the operator $C_\alpha^{[n-1]}$, and it is negative if $C_\alpha^{[n]}$ is a fermionic operator and the local state μ contains an odd number of fermions; otherwise it is positive. The local matrix elements ${}_{\text{loc}}\langle \mu | C_\alpha^{[n]} | \nu \rangle_{\text{loc}}$ are the same for all sites and can easily be determined, while ${}_{n-1}\langle u | C_\alpha^{[n-1]} | v \rangle_{n-1}$ can be computed from the previous iteration recursively. In fact, for any operator A , acting on sites $m < n$, and whose matrix elements are known in the iteration $n-1$, we have the following recursion relation:

$${}_n\langle\tilde{i}|A|\tilde{j}\rangle_n = {}_{n-1}\langle u|A|v\rangle_{n-1} F(a, \underline{Q}_{\tilde{i}}, \underline{Q}_{\tilde{j}}, \underline{Q}_u, \underline{Q}_v, \underline{q}_\mu) \delta_{\underline{q}_\mu, \underline{q}_v}, \quad (22)$$

where we can express the factor $F(a, \underline{Q}_{\tilde{i}}, \underline{Q}_{\tilde{j}}, \underline{Q}_u, \underline{Q}_v, \underline{q}_\mu)$ using Eq. (10) as

$$\begin{aligned} F(a, \underline{Q}_{\tilde{i}}, \underline{Q}_{\tilde{j}}, \underline{Q}_u, \underline{Q}_v, \underline{q}_\mu) &= \text{sgn}(A, \mu) \frac{1}{\dim(a)\dim(\tilde{j})} \sum_{\underline{Q}_{\tilde{i}}, \underline{Q}_{\tilde{j}}} \langle \underline{Q}_{\tilde{i}} \underline{Q}_{\tilde{j}} | a a^z; \underline{Q}_{\tilde{i}} \underline{Q}_{\tilde{j}} \rangle^* \sum_{\underline{Q}_u, \underline{Q}_v} \sum_{\underline{q}_\mu} \langle \underline{Q}_{\tilde{i}} \underline{Q}_{\tilde{j}} | \underline{q}_\mu \underline{q}_\mu^z; \underline{Q}_u \underline{Q}_v \rangle \\ &\times \langle \underline{Q}_{\tilde{i}} \underline{Q}_{\tilde{j}} | \underline{q}_\mu \underline{q}_\mu^z; \underline{Q}_v \underline{Q}_v \rangle^* \langle \underline{Q}_u \underline{Q}_u | a a^z; \underline{Q}_v \underline{Q}_v \rangle. \end{aligned} \quad (23)$$

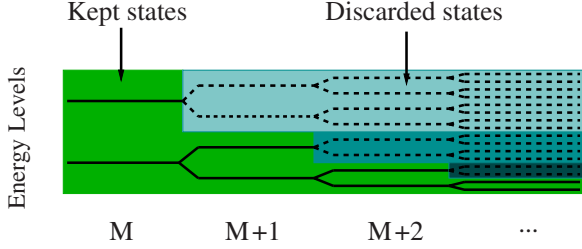


FIG. 2. (Color online) A complete basis of a Wilson chain represented as the exponentially increasing number of energy levels belonging to the successive iterations. Continuous/dashed lines represent kept, low-energy/discarded, high-energy levels, respectively. For the consecutive iteration steps the distances between the levels illustrate how the energy resolution of NRG gets exponentially refined.

One drawback of the algorithm above is that the eigenstates of H_n constructed this way do not form a complete basis of the Wilson chain of length n , since states descendant from the discarded states of the previous iteration are missing. However, as it was recently shown,¹⁷ one can construct a complete basis of the Wilson chain in a slightly different way. Let us consider a chain of length N , and construct approximate eigenstates of H_n with $n < N$ that, however, live at *all sites* of this chain,

$$|i, \underline{Q}_i \underline{Q}_i^z\rangle_n \rightarrow |i, \underline{Q}_i \underline{Q}_i^z; e\rangle_n. \quad (24)$$

In this equation, e just labels the d^{N-n} -independent “environment” states living at the last $N-n$ sites of the chain. The internal structure of these environment states is not important; only their degeneracies shall play some role. The previous iterative construction carries over to these states, too. By construction, discarded states (together with their environment state) form a complete basis set:

$$1 = \sum_{n=0}^N \sum_{i \in D} \sum_e \sum_{\underline{Q}_i^z} |i, \underline{Q}_i, \underline{Q}_i^z; e\rangle_{nm} \langle i, \underline{Q}_i, \underline{Q}_i^z; e|, \quad (25)$$

where $i \in D$ refers to the fact that *only discarded states* appear in the sum. In Eq. (25) in the last iteration at $n=N$ all states are considered discarded. We remark that, in the actual calculations, discarded states do not appear until the iteration $M > 0$ where the first truncation is carried out. Figure 2 illustrates the structure of this complete basis. In the formulation of the DM-NRG algorithm making use of non-Abelian symmetries we shall use several times the completeness relation, Eq. (25).

III. CONSTRUCTION OF THE REDUCED DENSITY MATRIX USING SYMMETRIES

In the DM-NRG procedure on a Wilson chain of length N , the equilibrium density matrix is approximated by¹⁹

$$\varrho = \sum_{n=0}^N \varrho^{[n]}, \quad (26)$$

$$\varrho^{[n]} = \sum_{\underline{Q}_i^z; i, e} \frac{e^{-\beta E_i^n}}{\mathcal{Z}} |i, \underline{Q}_i, \underline{Q}_i^z; e\rangle_{nm} \langle e; i, \underline{Q}_i, \underline{Q}_i^z|, \quad (27)$$

with $\beta = 1/k_B T$ as the Boltzmann factor and

$$\mathcal{Z} = \sum_{n=0}^N \sum_{\underline{Q}_i^z} e^{-\beta E_i^n} d^{N-n} \quad (28)$$

as the partition function.³⁰ In Eq. (28) the factor d^{N-n} accounts for the degeneracy of the environment states in iteration n , i.e., for the local degrees of freedom at sites $m > n$. Since the eigenenergies do not depend on the internal quantum numbers, the expression for the partition function can be simplified to

$$\mathcal{Z} = \sum_{n=0}^N \sum_i \dim(i) e^{-\beta E_i^n} d^{N-n}, \quad (29)$$

with the use of Eq. (10).

The concept of the reduced density matrix¹⁶ arises naturally as one starts to calculate Green’s functions with NRG. More precisely, the quantity that shows up in the calculations is the *truncated reduced density matrix*, defined as

$$R^{[n]} = \text{Tr} \left\{ \sum_{\{e_n\}_{m>n}} \varrho^{[m]} \right\}, \quad (30)$$

where one traces over environment states e_n at sites $m > n$. This truncated reduced density matrix clearly satisfies the recursion relations

$$R^{[N]} = \varrho^{[N]},$$

$$R^{[n-1]} = \text{Tr}_{\text{site } n} \{R^{[n]}\} + \sum_{i \in D} \frac{e^{-\beta E_i^{n-1, n-1}} d^{N-n+1}}{\mathcal{Z}} |i, \underline{Q}_i \underline{Q}_i^z\rangle_{n-1} \langle i, \underline{Q}_i \underline{Q}_i^z|. \quad (31)$$

Note that the environment variable is *missing* in the first term of the second expression since it has been traced over. The first term accounts for the contribution of discarded states, while the second term has matrix elements between the kept states only.

To construct the matrix elements of $R^{[n]}$ we first show by induction that $R^{[n]}$ is scalar under symmetry operations. This is clearly true for the first term in Eq. (31). To show that the second term is also invariant, we simply need to use the locality property of the symmetry transformations, i.e., that on the first n sites $U(g) \equiv L(g)V(g)$, where $L(g)$ transforms the local states on site n , while $V(g)$ transforms states at sites $0 \leq m \leq n-1$, and clearly, L and V commute with each other. Therefore, because of the invariance of the trace under cyclic permutations of the operators, we have

$$\begin{aligned} \text{Tr}_{\text{site } n} \{LVR^{[n]}V^+L^+\} &= \text{Tr}_{\text{site } n} \{VR^{[n]}V^+\} = V \text{Tr}_{\text{site } n} \{R^{[n]}\}V^+ \\ &= U \text{Tr}_{\text{site } n} \{R^{[n]}\}U^+. \end{aligned} \quad (32)$$

However, since $UR^{[n]}U^+ = R^{[n]}$ by assumption, we immediately obtain

$$\text{Tr}_{\text{site } n} \{R^{[n]}\} = U \text{Tr}_{\text{site } n} \{R^{[n]}\}U^+, \quad (33)$$

implying that

$$UR^{[n-1]}U^+ = R^{[n-1]} \quad (34)$$

for $R^{[n-1]}$, too. This equation means that $R^{[n]}$ is *scalar* and therefore, by the Wigner-Eckart theorem we have

$${}_n\langle i, \underline{Q}_i, \underline{Q}_i^z | R^{[n]} | j, \underline{Q}_j, \underline{Q}_j^z \rangle_n = {}_n\langle i | R^{[n]} | j \rangle_n \delta_{\underline{Q}_i, \underline{Q}_j} \delta_{\underline{Q}_i^z, \underline{Q}_j^z}. \quad (35)$$

The matrix elements ${}_n\langle i | R^{[n]} | j \rangle_n$ between discarded states simply derive from the first term in Eq. (31). To perform the trace in Eq. (31) and to construct the explicit relation between the kept matrix elements of $R^{[n-1]}$ and $R^{[n]}$ some more work is needed. First, we rotate $R^{[n]}$ to the canonical basis

$${}_n\langle \tilde{i} | \tilde{R}^{[n]} | \tilde{j} \rangle_n = \mathcal{O}_{\tilde{i}, i}^{[n]} {}_n\langle i | R^{[n]} | j \rangle_n (\mathcal{O}^{-1})_{\tilde{j}, j}^{[n]}. \quad (36)$$

Then, using the fact that $\text{Tr}_{\text{site } n} \{R^{[n]}\}$ is diagonal in the symmetry quantum numbers and labels, we can trace over the local states at site n using the recursion relation Eq. (13) to obtain the matrix elements between the kept states $u, v \in K$ as

$${}_{n-1}\langle u | R^{[n-1]} | v \rangle_{n-1} = \sum_{\tilde{i}, \tilde{j}, \underline{q}, \underline{\mu}, \underline{\mu}} \frac{\text{dim}(\tilde{i})}{\text{dim}(u)} {}_n\langle \tilde{i} | \tilde{R}^{[n]} | \tilde{j} \rangle_n \delta_{\underline{q}, \underline{\mu}} \delta_{\underline{\mu}, \underline{\mu}}. \quad (37)$$

Here the tilde over the sum indicates that in the summation over \tilde{i} and \tilde{j} only those states are considered which have been constructed from u ($\tilde{i} \leftarrow \underline{\mu}, u$) and v ($\tilde{j} \leftarrow \underline{\mu}, v$) in Eq. (13), respectively. This is a very powerful expression, which applies to essentially any type of discrete and compact Lie group symmetry.

IV. SPECTRAL FUNCTION COMPUTATION

The quantity that describes the linear response of a static system to a time-dependent perturbation and which is to be calculated in the DM-NRG framework is the retarded Green's function. For two irreducible tensor operators it is defined as

$$G_{A_{a, a_z}, B_{b, b_z}^\dagger}^R(t) = -i \langle [A_{a, a_z}(t), B_{b, b_z}^\dagger(0)] \Theta(t) \rangle. \quad (38)$$

By symmetry, however, this Green's function is nonzero only if the operators A and B transform according to the same representation, i.e.,

$$G_{A_{a, a_z}, B_{b, b_z}^\dagger}^R(t) = G_{A_{a, a_z}, B_{b, b_z}^\dagger}^R(t) \delta_{a, b} \delta_{a_z, b_z}, \quad (39)$$

and it is independent of the value of a_z and correspondingly of b_z . Note that in this expression the representation index b

and its labels b_z are the quantum numbers that characterize the operator B and not B^\dagger .

In the reduced density matrix formalism we can generalize the procedure outlined in Refs. 18 and 19 even in the presence of non-Abelian symmetries to obtain the following form for the Laplace transform of the Green's function:

$$\begin{aligned} G_{A, B^\dagger}^R(z) &= \sum_{n=0}^N \sum_{i \in D, K} \sum_{(j, k) \in (K, K)} {}_n\langle i | R^{[n]} | j \rangle_n \\ &\times \left[\frac{{}_n\langle k | A^\dagger | j \rangle_n \langle k | B^\dagger | i \rangle_n \text{dim}(k)}{z + \frac{1}{2}(E_i^n + E_j^n) - E_k^n} \frac{\text{dim}(a)}{\text{dim}(a)} \right. \\ &\left. - \xi^n \frac{{}_n\langle j | B^\dagger | k \rangle_n \langle i | A^\dagger | k \rangle_n \text{dim}(i)}{z - \frac{1}{2}(E_i^n + E_j^n) - E_k^n} \frac{\text{dim}(i)}{\text{dim}(a)} \right]. \end{aligned} \quad (40)$$

Remarkably, this formula contains exclusively the reduced matrix elements and the dimensions of the various multiplets. Here the second sum is over all the multiplets i, j, k of the given iteration subject to the restriction that j, k do not belong to kept states at the same time and no summation is needed for states within the multiplets. In Eq. (40), $\text{dim}(a) = \prod_{\gamma=1}^{\Gamma} \text{dim}(a^\gamma)$ is the dimension of the operator multiplet A_{a, a_z} . We note that the irreducible matrix elements of $R^{[n]}$ are identical with the original ones since $R^{[n]}$ is invariant under all symmetry transformations; i.e., it is a rank 0 object with respect to all symmetries. Equation (40) explicitly shows that $G_{A, B^\dagger}^R(z) = 0$ unless A and B have the same quantum numbers (i.e., $a = b$).

V. NUMERICAL RESULTS

In this section we show the advantages of using DM-NRG as opposed to NRG and illustrate the benefits of using non-Abelian symmetries by applying DM-NRG to the 2CK model. This model is exciting in itself as it possesses a non-Fermi-liquid type of fixed point and it provides the simplest descriptions of the double-dot system used recently to realize the 2CK state.²⁵ This 2CK state is very fragile and in a magnetic field the difference between the NRG and DM-NRG results is substantial.

In the Wilson approach, the 2CKM is described by the following Hamiltonian:

$$\begin{aligned} H_{2\text{CK}} &= \frac{1}{2} \tilde{S} \sum_{\alpha \in \{1, 2\}} \mathcal{J}_\alpha \sum_{\mu, \nu \in \{\uparrow, \downarrow\}} f_{0, \alpha, \mu}^\dagger \tilde{\sigma}_{\mu\nu} f_{0, \alpha, \nu} \\ &+ \sum_{n=0}^{\infty} \sum_{\alpha \in \{1, 2\}} \sum_{\mu \in \{\uparrow, \downarrow\}} t_n (f_{n, \alpha, \mu}^\dagger f_{n, \alpha, \mu} + \text{H.c.}), \end{aligned} \quad (41)$$

where we have introduced $\alpha \in \{1, 2\}$ for labeling the two types of electrons. This additional channel label is the only difference compared to the one-channel Kondo Hamiltonian [cf. Eq. (A1)].^{10, 24}

TABLE I. Symmetry generators of the single-channel Kondo model. Sites along the Wilson chain are labeled by n and $C^+ = \sum_{n=0}^{\infty} (-1)^n f_{n,\uparrow}^\dagger f_{n,\downarrow}^\dagger$.

Symmetry group	Generators (\vec{g})		
$SU_S(2)$	$\vec{S}_T = \vec{S} + 1/2 \sum_{n=0}^{\infty} \sum_{\mu,\nu \in \{\uparrow,\downarrow\}} f_{n,\mu}^\dagger \vec{\sigma}_{\mu,\nu} f_{n,\nu}$		
$SU_{C_1}(2)$	$C^x = [C^+ + (C^+)^\dagger]/2$	$C^y = [C^+ - (C^+)^\dagger]/2i$	$C^z = 1/2 \sum_{n=0}^{\infty} (\sum_{\mu \in \{\uparrow,\downarrow\}} f_{n,\mu}^\dagger f_{n,\mu} - 1)$

In this model, the number of carriers is conserved in both channels corresponding to a $U_{C_1}(1) \times U_{C_2}(1)$ symmetry. However, due to the presence of electron-hole symmetry, these charge symmetries are augmented to $SU(2)$ symmetries, and the Hamiltonian above is also invariant under $SU_S(2) \times SU_{C_1}(2) \times SU_{C_2}(2)$ transformations. On the other hand, one can solve this Hamiltonian using exclusively $U(1)$ symmetries, $U_S(1) \times U_{C_1}(1) \times U_{C_2}(1)$. This model is thus ideal for testing our flexible methods.

If a local magnetic field is coupled to the impurity spin through a term $g\mu_B B S_z^c$, from among the total spin generators (see Table I) solely S_z^c will commute with the Hamiltonian. That is, the spin $SU(2)$ symmetry of the system reduces to $U(1)$. Therefore, in a magnetic field we can either use the symmetry $U_S(1) \times SU_{C_1}(2) \times SU_{C_2}(2)$ for our calculations, or restrict ourselves to $U(1)$ symmetries only: $U_S(1) \times U_{C_1}(1) \times U_{C_2}(1)$.

As a test, we computed the retarded Green's function $G_{f_{0,\alpha,\uparrow}^\dagger}^R(\omega)$ and the corresponding spectral function $\rho_{f_{0,\alpha,\uparrow}^\dagger}(\omega)$ both in the presence and in the absence of magnetic field. All numerical results presented were obtained at zero temperature, and the dimensionless couplings were $\mathcal{J}_\alpha = 0.2$ for both channels and all runs. The discretization parameter $\Lambda = 2$ was used in all cases, and for each symmetry combination we have retained a maximum number of 1350 multiplets in each iteration.

In Fig. 3 we show data for the local fermion's spectral function in the absence of magnetic field obtained through the NRG and the DM-NRG approaches using the two symmetry groups mentioned above. The Kondo scale T_K in Fig. 3 is the scale at which the 2CK state forms, and it is defined as the frequency where the T matrix of the 2CK model drops to half of its value assumed at $\omega = 0$ at the 2CK fixed point.³¹

The first important test is the fulfillment of the spectral sum rules. These are always satisfied in the DM-NRG calculations independently of the symmetry group used, whereas the NRG data violate the sum rule to over 15% if the number of kept multiplets is 1350 corresponding to $\approx 7 \times 10^4$ states. Figure 3(b) shows that the expected $\sqrt{\omega}$ behavior around the 2CK fixed point is nicely recovered by both methods, but a sufficiently large number of multiplets must be kept also in the DM-NRG approach, meaning that in this case the larger symmetry group must be used. Figure 3(c) demonstrates that in spite of fulfilling the spectral sum rules still the DM-NRG data do not show the expected asymptotics for low frequencies if the number of multiplets kept is not sufficient. It is quite remarkable that only the DM-NRG procedure using non-Abelian symmetries was able to get close to the exact

value of the spectral function at $\omega = 0$ and $\rho_{f_{0,\alpha,\uparrow}^\dagger}(\omega = 0) = 0.25$.³² The presence of magnetic field generates a new scale,³

$$T_h \equiv C_h \frac{B^2}{T_K}, \quad (42)$$

where we have fixed the somewhat arbitrary constant to $C_h \approx 60$.³³ This scale is usually referred to as the renormalized magnetic field acting on the impurity, and below this scale the non-Fermi-liquid physics is destroyed.

In the presence of magnetic field the sum rule is violated by the NRG approach to a different extent in the positive and

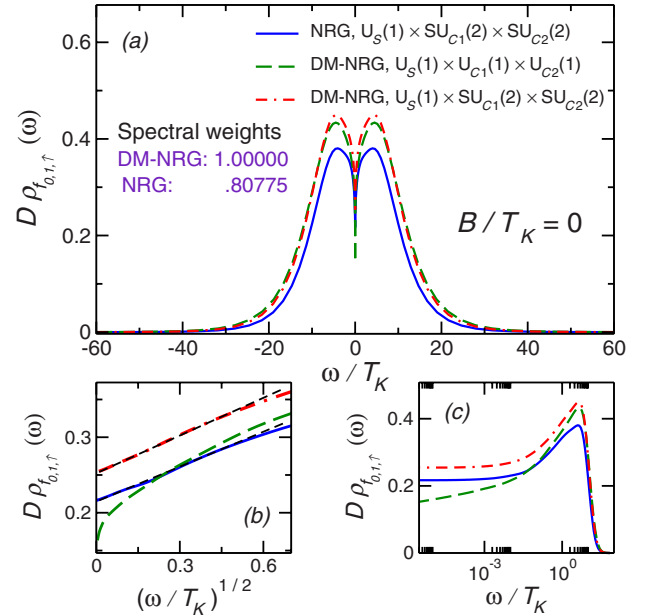


FIG. 3. (Color online) Dimensionless spectral function of $f_{0,1,\uparrow}$ normalized by D , the bandwidth cutoff, as a function of ω/T_K in the absence of magnetic field obtained with DM-NRG and with NRG using the symmetries: $U_S(1) \times SU_{C_1}(2) \times SU_{C_2}(2)$ and $U_S(1) \times U_{C_1}(1) \times U_{C_2}(1)$. (a) Comparison between the spectral weights of the DM-NRG and NRG results: DM-NRG fulfills the sum rule entirely even when the used symmetry group and therefore the number of kept states is largely reduced. NRG violates the sum rule to over 15% if the number of kept states is $\approx 7 \times 10^4$ in each iteration. (b) The same spectral functions as a function of $\sqrt{\omega/T_K}$. If a sufficient number of states is kept, i.e., when using larger symmetry groups, the expected $\sqrt{\omega}$ behavior around the 2CK fixed point is nicely recovered. (c) The same spectral functions on a logarithmic scale.

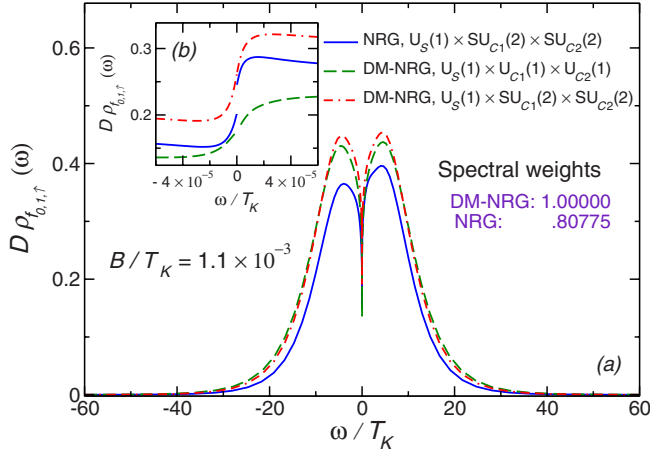


FIG. 4. (Color online) Dimensionless spectral function of $f_{0,1,\uparrow}$ normalized by D , the bandwidth cutoff, as a function of ω/T_K in the presence of magnetic field obtained with DM-NRG and with NRG using the symmetries: $U_S(1) \times SU_{C1}(2) \times SU_{C2}(2)$ and $U_S(1) \times U_{C1}(1) \times U_{C2}(1)$. (b) On a smaller scale at $\omega=0$ we show the smoothness of the DM-NRG data using both groups and the jump at $\omega=0$ in the NRG results using the larger group.

negative frequency ranges, which leads to jumps at $\omega=0$ in the spectral functions (see Fig. 4), while this problem is absent in the DM-NRG approach. Spectral functions display universal scaling in the vicinity of T_h .³³ In Fig. 5 we show how the spectral functions of the composite fermion operator

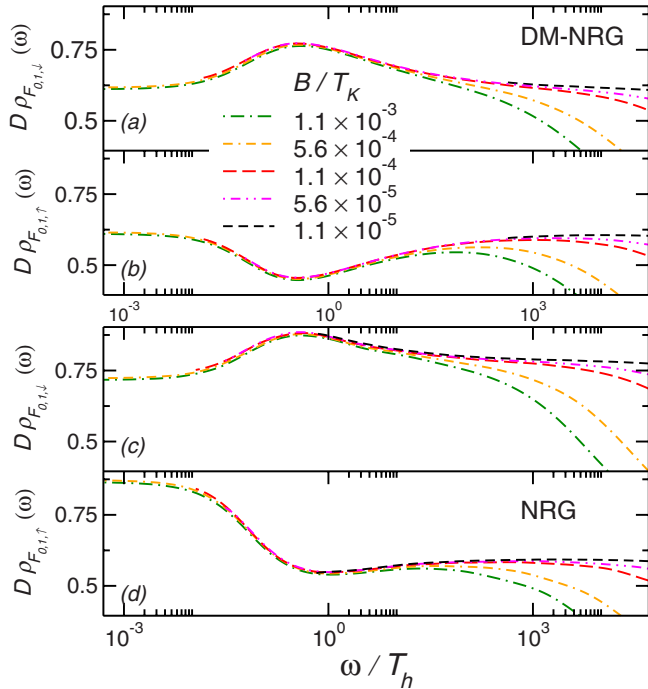


FIG. 5. (Color online) Dimensionless spectral function of [(a) and (c)] the \downarrow - and [(b) and (d)] the \uparrow -spin components of the local composite fermion operator normalized by D , the bandwidth cutoff, for sufficiently small values of B as a function of ω/T_h scaled on top of each other using NRG and DM-NRG together with the group $U_S(1) \times SU_{C1}(2) \times SU_{C2}(2)$.

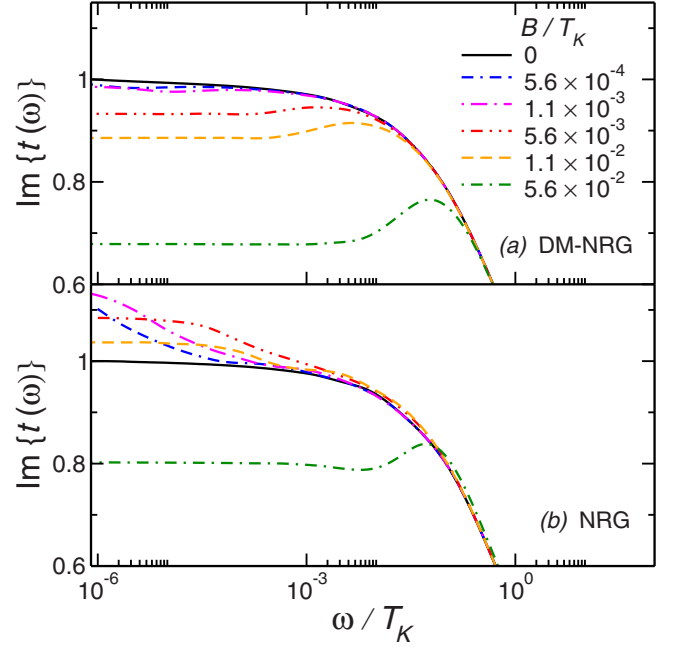


FIG. 6. (Color online) Imaginary part of the on-shell T matrix using DM-NRG and NRG together with the group $U_S(1) \times SU_{C1}(2) \times SU_{C2}(2)$ for various magnetic-field values as a function of ω/T_K .

$F_1^\dagger \equiv f_{0,1}^\dagger \vec{S} \vec{\sigma}$ can be scaled on top of each other using the scale T_h . Although this collapse can be obtained in both approaches, there is an $\approx 20\%$ jump at $\omega=0$ in the NRG results while the DM-NRG results are continuous there. It is possible to eliminate the jump in the NRG results by determining the phase shifts from the energy spectrum with high precision, but even after these corrections, the results continue to violate the sum rule and numerical errors for low frequencies remain of the same size as before. Moreover, the “universal” curve obtained by conventional NRG is clearly incorrect and different from the DM-NRG result. Also, if we try to compute the imaginary part of the on-shell T matrix of the 2CK model where the local composite fermion spectral functions for both \uparrow - and \downarrow -spin components have to be summed up, we end up with large numerical errors in the NRG results (see Fig. 6), while DM-NRG provides satisfactory results even in this case.

As a final example, we present results for the energy dependent spin polarized conductance. We define the polarization as

$$P(\omega) \equiv \frac{\text{Re } G_\uparrow(\omega) - \text{Re } G_\downarrow(\omega)}{\text{Re } G_\uparrow(\omega) + \text{Re } G_\downarrow(\omega)}, \quad (43)$$

with $\text{Re } G_\sigma(\omega)$ as the real part of the spin-dependent linear dynamical conductance (see Fig. 7). The frequency-dependent (ac) conductance is closely related to the spectral function of the composite fermion operator, which exhibits a universal peak structure in a magnetic field.³¹ Therefore a corresponding peak is also expected in $P(\omega)$ at $\omega \approx T_h$. Indeed, both the DM-NRG and the NRG methods give a polarization with a sharp structure at $\omega \approx T_h$.

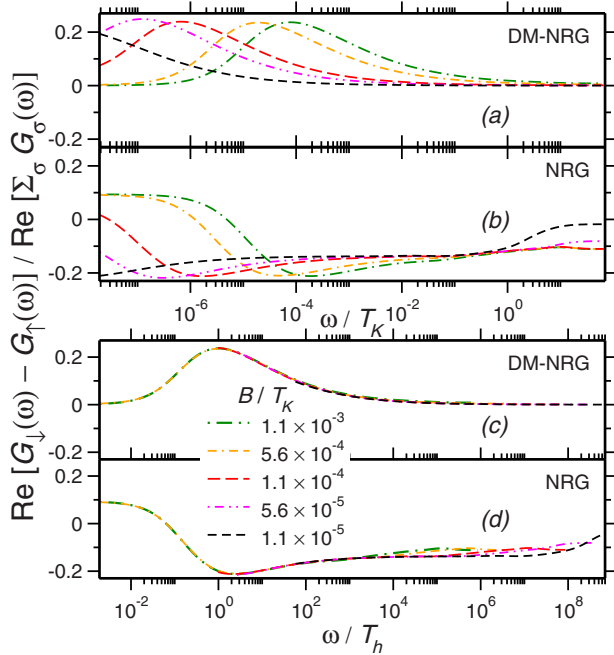


FIG. 7. (Color online) Polarization in the 2CKM as a function of ω/T_K computed by (a) DM-NRG and by (b) NRG, and the same quantity as a function of ω/T_h showing universal behavior for small ω , but completely contradicting each other as computed by (c) DM-NRG and by (d) NRG.

In the DM-NRG calculations, the nice symmetrical peaks and dips in \mathcal{Q}_{F_\uparrow} and $\mathcal{Q}_{F_\downarrow}$ give a clear resonance in the polarization, which vanishes for large frequencies. It is rather remarkable that the shape of this resonance is completely universal when plotted against ω/T_h : the width of it is $\Delta\omega \propto T_h$, while its height is independent of T_h . Thus, even with an infinitesimally small magnetic field, a large polarization, $P \approx 0.2$, can be reached if the frequency of the voltage is properly adjusted, while the total conductance remains very close to half of the maximum conductance, $G_\uparrow + G_\downarrow \approx e^2/h$.

Notice that in the single-channel Kondo model no such universal peak appears in a small magnetic field, and only magnetic fields on the order of T_K have influence on the low-frequency behavior of the composite fermion's spectral function and lead to the well-known splitting of the Kondo resonance.³⁴ This universal resonance in the polarization is thus a peculiar feature of the two-channel Kondo state, and probably also of other non-Fermi-liquid states and quantum impurity models.

In contrast to DM-NRG, the NRG calculation is unable to properly capture this resonant feature: due to the difference in spectral losses for the $\sigma=\uparrow$ and $\sigma=\downarrow$ components, the NRG method obviously leads to incorrect results, and misses not only the shape and high frequency value of the polarization, but even the overall sign of the polarization. It is thus clear from these examples that the DM-NRG method together with the use of a lot of symmetries produces much more reliable results than NRG with non-Abelian symmetries or DM-NRG with only Abelian symmetries, and its use is needed to do computations for more delicate quantum impurity models.

VI. CONCLUSIONS

To summarize, in this paper, we have shown how the recently developed spectral sum-conserving DM-NRG methods can be used in the presence of any number and type of discrete and compact Lie group symmetries. The most important result of this paper is a very general and simple recursion relation for the truncated reduced density matrix, which enables us to compute the spectral properties of any local correlation function in the presence of non-Abelian symmetries. The expressions derived hold for almost any symmetry, including non-Abelian finite groups, point groups, $SU(N)$ groups, and, of course, Abelian groups such as $U(1)$ or the parity. The use of these symmetries reduces considerably the time needed for the computations and enhances significantly the accuracy of the numerical results for dynamical quantities. The general formulation presented in this paper also allowed us to construct a flexible DM-NRG code where symmetries are handled dynamically, and which is able to learn and handle essentially any type of symmetry.²³

We demonstrated the advantages of the generalized method by applying it to the two-channel Kondo model in magnetic field. The presence of magnetic field makes this model very challenging from the point of view of NRG calculations. We have carried out calculations for the local fermion's and for the local composite fermion's spectral function at zero temperature and in finite magnetic field. In conventional NRG, there is always a jump at $\omega \rightarrow 0$ between the positive and negative frequency parts of the spectral function. In addition to being spectral sum-conserving, the use of DM-NRG eliminated this jump almost completely and made it possible to compute the universal crossover curves in magnetic field. Moreover, the DM-NRG approach used with larger symmetry groups has provided substantially better results for the spectral functions: in the limit $\omega \rightarrow 0$ we needed to use non-Abelian symmetries in the DM-NRG approach to recover the expected power-law behavior known from conformal field theory. Also, the universal crossover curve and the shape of the peak at the renormalized magnetic field $T_h \propto B^2/T_K$ was much better resolved by DM-NRG than by NRG, and thus DM-NRG with non-Abelian symmetries led to much more reliable results for the T matrix (see Fig. 5) than NRG with non-Abelian or DM-NRG with Abelian symmetries. We emphasize that to obtain the $\omega=0$ value of the spectral function correctly as well as its proper scaling behavior, we needed to use non-Abelian symmetries.

As an application, we also discussed the spin polarization of the frequency-dependent conductance through a quantum dot in the two-channel Kondo regime.²⁵ We have shown that a sharp, universal resonance appears in the polarization at the frequency, $\omega \sim T_h \sim B^2/T_K$. Remarkably, at $T=0$ temperature the polarization of the current remains finite at the resonance ($P \approx 0.2$) even in the limit of *vanishing* external field, $B \rightarrow 0$, while the total conductance remains finite.

The method presented here thus opens up the possibility to carry out very accurate spectral sum-conserving DM-NRG calculations for multichannel systems, such as multidot devices, and to perform reliable DM-NRG-DMFT calculations for multichannel lattice models. Combined with the matrix product state approach, it might also provide a way to use

methods applied in DMRG to improve the high frequency resolution of NRG.

ACKNOWLEDGMENTS

We are deeply indebted to Ireneusz Weymann, who participated in the initial stage of the construction of the flexible NRG code, and to László Borda for his help and many comments. We are indebted to Jan von Delft for the numerous valuable remarks made on the manuscript. We would like to thank Frithjof Anders and Andreas Weichselbaum for useful discussions. This research was supported partly by the Hungarian Research Fund (OTKA) under Grants No. NF 61726 and No. K 68340, and by the János Bolyai Research Fund. A.T. is grateful to the Institute of Mathematics of BUTE for providing access to their computer supported by OTKA under Grant No. NK 63066. A.T. was also partially supported by the Landesstiftung Baden-Württemberg via the Kompetenznetz Funktionelle Nanostrukturen. C.P.M. was partially supported by the Romanian CNCSIS under Grant No. 1/780/2008.

APPENDIX A: SYMMETRIES OF THE ONE-CHANNEL KONDO MODEL

To be more specific, in this appendix we demonstrate how the general formalism introduced in Sec. II works for the 1CKM. In the NRG procedure, Wilson used the following approximation for the 1CK Hamiltonian:¹⁰

$$H_{1\text{CK}} = \frac{1}{2} \mathcal{J} \sum_{\mu, \nu \in \{\uparrow, \downarrow\}} \vec{S}_{0, \mu}^{\dagger} \vec{\sigma}_{\mu} f_{0, \nu} + \sum_{n=0}^{\infty} \sum_{\mu \in \{\uparrow, \downarrow\}} t_n (f_{n, \mu}^{\dagger} f_{n+1, \mu} + \text{H.c.}), \quad (\text{A1})$$

with $f_{0, \mu}^{\dagger}$ creating a conduction electron of spin σ at the impurity site, \vec{S} as the impurity spin, and \mathcal{J} as the exchange coupling. The kinetic part of the Hamiltonian is described by the semi-infinite Wilson chain. Electrons (fermions) move along this chain with exponentially decreasing hopping amplitudes, $t_n \propto \Lambda^{-n/2}$, with Λ as the discretization parameter.¹⁰

The above model has various symmetries; i.e., it is invariant under unitary transformations,

$$H_{1\text{CK}} = \mathcal{U} H_{1\text{CK}} \mathcal{U}^{\dagger}, \quad (\text{A2})$$

where the unitary operator \mathcal{U} is generated by

$$\mathcal{U} \equiv \mathcal{U}(\vec{\omega}) = e^{i\vec{\omega}\vec{g}}, \quad (\text{A3})$$

with generators \vec{g} listed in Table I and parametrized by real, three-component vectors $\vec{\omega}$.

Since the spin symmetry generators commute with the charge symmetry generators, $H_{1\text{CK}}$ possesses a symmetry, $\text{SU}_S(2) \times \text{SU}_C(2)$,³⁵ and consequently, the eigenstates of the Hamiltonian form degenerate multiplets, $|i, \underline{Q}_i, Q_i^z\rangle$, that are classified by their multiplet label i , the spin and charge quantum numbers $\underline{Q}_i \equiv \{S_i, C_i\}$,³⁶ and the z components of the spin and charge operators, $Q_i^z \equiv \{S_i^z, C_i^z\}$. We use the convention

that every multiplet in the spectrum is labeled by a separate label i just as was introduced in Sec. II.

Now the dimension of the i th irreducible subspace is given as $\dim(i) = \dim(Q_i) = (2S_i + 1)(2C_i + 1)$. One of the simplest examples for an irreducible tensor operator multiplet²⁸ is provided by the impurity spin, from the components of which we can form the operator triplet as

$$\{A_m\} \equiv \left\{ -\frac{1}{\sqrt{2}} S^+, S^z, \frac{1}{\sqrt{2}} S^- \right\}. \quad (\text{A4})$$

The components of this triplet transform under spin rotations as the eigenstates $|m\rangle$ of S^z , while they are invariant under charge rotations. This means that A has quantum numbers, $S_A = 1$ and $C_A = 0$, and the components of this operator multiplet are labeled by $S_A^z = m$, ($m = 0, \pm 1$), while the internal charge label is trivially $C_A^z = 0$. Similar to the eigenstates of the Hamiltonian, in our simple example the quantum numbers of an irreducible tensor operator B can be organized into a representation index vector, $\underline{b} = (S_B, C_B)$, and the components of B are labeled by $b^z = (S_B^z, C_B^z)$ taking the values $S_B^z = -S_B, -S_B + 1, \dots, S_B$ and $C_B^z = -C_B, -C_B + 1, \dots, C_B$. A further example for an $S = 1/2$ and $C = 1/2$ operator is formed by the four operators $\{f_{0, \uparrow}^{\dagger}, f_{0, \downarrow}^{\dagger}, f_{0, \downarrow}, -f_{0, \uparrow}\}$.

APPENDIX B: PROOF OF THE DIAGONAL FORM OF THE REDUCED DENSITY MATRIX FOR $\text{SU}(2)$ SYMMETRIES

In this appendix we prove, in a different way from how it was demonstrated in the main part of the paper, the general theorem for the diagonal form of the reduced density matrix presented in Sec. III in the case when only $\text{SU}(2)$ local symmetries are involved. The proof for the diagonal form of the reduced density matrix goes by induction for the iteration steps. At the last iteration, by construction the reduced density matrix $R^{[N]}$ is scalar under the local symmetry group [cf. Eq. (31)]. Due to this invariance by very general considerations $R^{[N]}$ can be written as a sum over tensor products of irreducible tensor operator components, and is of the form

$$R^{[N]} = \sum_{\alpha} (T_{\alpha}^{[\text{loc}]})_{\underline{l}, \underline{l}^z}^{\dagger} \otimes (T_{\alpha}^{[N-1]})_{\underline{l}, \underline{l}^z}, \quad (\text{B1})$$

where $(T_{\alpha}^{[\text{loc}]})_{\underline{l}, \underline{l}^z}$ and $(T_{\alpha}^{[N-1]})_{\underline{l}, \underline{l}^z}$ are irreducible tensor operator components of the same rank \underline{l} acting on the local vector space at site N and on the rest of the Wilson chain, respectively, and α labels all possible tensor operators. This special form is a consequence of the invariance of $R^{[N]}$ under the local symmetry transformations.³⁷

To obtain $R_{KK}^{[N-1]}$ we have to trace over the local basis states, $\{|\mu, q_{\mu}, q_{\mu}^z\rangle_{\text{loc}}\}$, that is we have to compute the following matrix elements:

$$\begin{aligned}
\langle u || R_{KK}^{[N-1]} || v \rangle &= \sum_{\alpha, q_\mu \mu} \text{sgn}(T_\alpha^{[N-1]}, q_\mu) \\
&\times \langle u || T_\alpha^{[N-1]} || v \rangle \langle \mu || T_\alpha^{[\text{loc}]} || \mu \rangle \\
&\times \langle \underline{Q}_u \underline{Q}_u^z | \underline{t}^z; \underline{Q}_v \underline{Q}_v^z \rangle \sum_{q_\mu^z = -q_\mu}^{q_\mu} \langle q_\mu q_\mu^z | \underline{t}^z; q_\mu q_\mu^z \rangle.
\end{aligned} \tag{B2}$$

In Eq. (B2) we have applied the Wigner-Eckart theorem. The sign factor $\text{sgn}(\dots)$ depends on the number of fermionic operators used in the construction of $T_\alpha^{[N-1]}$ and the local

states. In Eq. (B2) only the terms with $t_z=0$ give nonvanishing contributions and the last sum can be reduced by using

$$\sum_{q^z=-q}^q \langle qq^z | t_0 qq^z \rangle = (2q+1) \delta_{t,0}. \tag{B3}$$

Equation (B3) implies that the only nonvanishing contributions are those corresponding to $t_z=0$, i.e., to scalar $T_\alpha^{[\text{loc}]}$ and $T_\alpha^{[N-1]}$. Therefore the reduced density matrix $R^{[N-1]}$ is diagonal in the representation indices. The induction toward smaller iteration steps goes recursively the same way.

-
- ¹For a review, see, e.g., L. I. Glazman and M. Pustilnik, in *Nanophysics: Coherence and Transport*, edited by H. Bouchiat, S. Guéron, Y. Gefen, G. Montambaux, and J. Dalibard (Elsevier, New York, 2005), pp. 427–478.
- ²A. Georges, G. Kotliar, W. Krauth, and M. J. Rozenberg, *Rev. Mod. Phys.* **68**, 13 (1996).
- ³N. Andrei and C. Destri, *Phys. Rev. Lett.* **52**, 364 (1984).
- ⁴A. M. Tsvetick and P. B. Wiegmann, *J. Stat. Phys.* **38**, 125 (1985).
- ⁵I. Affleck and A. W. W. Ludwig, *Nucl. Phys. B* **352**, 849 (1991); **360**, 641 (1991); I. Affleck, A. W. W. Ludwig, H. B. Pang, and D. L. Cox, *Phys. Rev. B* **45**, 7918 (1992).
- ⁶V. J. Emery and S. Kivelson, *Phys. Rev. B* **46**, 10812 (1992).
- ⁷A. A. Abrikosov, *Physics* (Long Island City, N.Y.) **2**, 5 (1965).
- ⁸M. Fowler and A. Zawadowski, *Solid State Commun.* **9**, 471 (1971).
- ⁹Ph. Nozières, *J. Low Temp. Phys.* **17**, 31 (1974).
- ¹⁰K. G. Wilson, *Rev. Mod. Phys.* **47**, 773 (1975); for a recent review of NRG, see R. Bulla, T. Costi, and T. Pruschke, *ibid.* **80**, 395 (2008).
- ¹¹L. N. Oliveira and J. W. Wilkins, *Phys. Rev. B* **24**, 4863 (1981); **32**, 696 (1985).
- ¹²T. A. Costi and A. C. Hewson, *Philos. Mag. B* **65**, 1165 (1992).
- ¹³T. A. Costi, A. C. Hewson, and V. Zlatić, *J. Phys.: Condens. Matter* **6**, 2519 (1994).
- ¹⁴S. Suzuki, O. Sakai, and Y. Shimizu, *J. Phys. Soc. Jpn.* **65**, 4034 (1996).
- ¹⁵S. R. White, *Phys. Rev. Lett.* **69**, 2863 (1992); *Phys. Rev. B* **48**, 10345 (1993).
- ¹⁶W. Hofstetter, *Phys. Rev. Lett.* **85**, 1508 (2000).
- ¹⁷F. B. Anders and A. Schiller, *Phys. Rev. Lett.* **95**, 196801 (2005).
- ¹⁸R. Peters, T. Pruschke, and F. B. Anders, *Phys. Rev. B* **74**, 245114 (2006).
- ¹⁹A. Weichselbaum and J. von Delft, *Phys. Rev. Lett.* **99**, 076402 (2007).
- ²⁰R. Žitko and J. Bonca, *Phys. Rev. B* **73**, 035332 (2006).
- ²¹I. P. McCulloch and M. Gulácsi, *Europhys. Lett.* **57**, 852 (2002).
- ²²U. Schollwöck, *Rev. Mod. Phys.* **77**, 259 (2005).
- ²³This code has open access and is accessible at the site <http://www.phy.bme.hu/~dmnrg>; for a comprehensive manual, see O. Legeza, C. P. Moca, A. I. Toth, I. Weymann, and G. Zarand, arXiv:0809.3143 (unpublished).
- ²⁴D. L. Cox and A. Zawadowski, *Adv. Phys.* **47**, 599 (1998).
- ²⁵R. M. Potok, I. G. Rau, H. Shtrikman, Y. Oreg, and D. Goldhaber-Gordon, *Nature* (London) **446**, 167 (2007).
- ²⁶For groups like SU(3), having a more complicated Cartan subalgebra, every component of the internal labels $Q^{i,z}$ is composed of several quantum numbers.
- ²⁷One could also use a convention where the states of a given quantum number are distinguished by separate labels.
- ²⁸J. F. Cornwell, *Group Theory in Physics, An Introduction* (Academic, New York, 1997).
- ²⁹Some of the considerations presented here do not carry over for noncompact Lie groups.
- ³⁰Approximations also exist in the literature, e.g., the one in Ref. 17 where Q comes only from the last iteration.
- ³¹A. I. Tóth, L. Borda, J. von Delft, and G. Zarand, *Phys. Rev. B* **76**, 155318 (2007).
- ³²One can show that $\rho_{f_{0,\alpha,\uparrow}} = \frac{1}{2}\rho_0 = \frac{1}{4}$ at the 2CK fixed point, in the large bandwidth limit. This follows from a theorem of Maldacena and Ludwig who proved that the single-particle S matrix vanishes at the 2CK fixed point, and from the relation between the Green's function of the local fermion $f_{0,\alpha,\uparrow}$ and the T matrix; see, e.g., Eq. (30) of Ref. 33.
- ³³A. I. Tóth and G. Zarand, *Phys. Rev. B* **78**, 165130 (2008).
- ³⁴T. A. Costi, *Phys. Rev. B* **64**, 241310(R) (2001).
- ³⁵B. A. Jones, C. M. Varma, and J. W. Wilkins, *Phys. Rev. Lett.* **61**, 125 (1988).
- ³⁶The eigenvalues of the operators \vec{S}^2 and \vec{C}^2 are given by $S(S+1)$, $C(C+1)$.
- ³⁷A. I. Tóth, Ph.D. thesis, Budapest University of Technology and Economics, 2009.